J Membrane Biol (2015) 248:171–178
DOI 10.1007/s00232-014-9754-9

ORIGINAL ARTICLES

Increase in Neuropilin-1 on the Surface of Growth Cones and Putative Raft Domains in Neuronal NG108-15 Cells Co-Cultured with Vascular Smooth Muscle SM-3 Cells

Ryoichi Yoshimura · Ayumi Kyuka · Miwa Jinno · Satomi Nishio · Mamoru Matsusaka · Tomoki Nishida · Yasuhisa Endo

Received: 2 September 2014 / Accepted: 11 November 2014 / Published online: 22 November 2014

Abstract The mechanisms underlying autonomic innervation to its targets involve various chemical factors, but have not yet been elucidated in detail. We constructed a co-culture system of neuronal cells and vascular smooth muscle cells to investigate the mechanisms underlying innervation of the vasculature. A co-culture with the vascular smooth muscle cell line, SM-3 significantly promoted cell viability, neurite extension, and neuropilin-1 (Nrp-1) mRNA expression in the cholinergic neuronal cell line, NG108-15. Furthermore, immunocytochemistry with or without a detergent treatment revealed that a co-culture with SM-3 cells or culturing with the conditioned medium of SM-3 cells translocated Nrp-1 onto the cell surface of growth cones rather than varicosities of NG108-15 cells. Immunofluorescent microscopy combined with a cold detergent treatment or cholesterol depletion revealed that Nrp-1 accumulated in putative raft domains in the plasma membrane of NG108-15 cells co-cultured with SM-3 cells. The results of the present study suggest that some soluble factors from smooth muscle cells may affect the localization of Nrp-1 in cholinergic neuronal cells, which may, in turn, be involved in the autonomic innervation of blood vessels.

Keywords Co-culture · Autonomic vascular innervation · Axon repellent · Lipid raft · Membrane protein extraction

R. Yoshimura (✉) · A. Kyuka · M. Jinno · S. Nishio · M. Matsusaka · Y. Endo
Department of Applied Biology, Kyoto Institute of Technology, Matsugasaki, Sakyo-Ku, Kyoto 606-8585, Japan
e-mail: ryoshimu@kit.ac.jp

T. Nishida
Research Center for Ultra-High Voltage Electron Microscopy, Osaka University, Mihogaoka, Ibaraki, Osaka, Japan

Introduction

The autonomic nervous system controls the heart, endocrine, and exocrine glands as well as the smooth muscle cells of these glands, blood vessels, and other internal organs. The autonomic postganglionic innervation of blood vessels is an important determinant of cardiovascular function. Autonomic nerves have been proposed to follow vascular smooth muscle, the endothelium, or basal laminae. Although the mechanisms underlying autonomic innervation to its targets are known to involve artemin, endothelin-3, nerve growth factor, neurotrophin-3, netrin-1, semaphorin 3A (Sema3A), and vascular endothelial growth factors (VEGFs), they have not yet been elucidated in detail (Bates et al. 2003; Brunet et al. 2014; Enomoto et al. 2001; Honma et al. 2002; Kuruvilla et al. 2004; Long et al. 2009; Makita et al. 2008; Marko and Damon 2008). Previous studies reported that axon guidance was mediated by extracellular attractive and repulsive cues through membrane microdomains, the so-called lipid rafts, on growth cones, which are enriched with cholesterol and sphingolipids and are resistant to cold detergent extraction (Grider et al. 2009; Guirland and Zheng 2007; Hooper 1999; Kamiguchi 2006; Simons and Ikonen 1997). The repulsion of neurites may involve Sema3A and neuropilin-1 (Nrp-1), one of its receptors.

Nrp-1 is a membrane-spanning co-receptor to one of the plexins or VEGF receptors for both VEGF and semaphorin family members. Nrp-1 has been shown to play a wide range of roles in angiogenesis, axon guidance, cell survival, invasion, and migration (Fujisawa et al. 1997; He and Tessier-Lavigne 1997; Kitsukawa et al. 1997; Kolodkin et al. 1997; Marko and Damon 2008).

Lipid rafts are cholesterol-rich glycolipoprotein microdomains in the plasma membrane. These specialized membrane microdomains mediate cellular processes by serving as

gathering sites for the condensation of signaling molecules, restricting membrane fluidity and membrane protein trafficking, and regulating neurotransmission and receptor signal transduction (Foster et al. 2003; Pike and Miller 1998; Simons and Ikonen 1997; Verkade and Simons 1997).

Cold Triton X-100 (TX-100) treatments have been used to extract membrane proteins at sites except for lipid rafts, whereas cholesterol depletion by methyl-beta-cyclodextrin (MBCD) perturbs cholesterol-rich rafts and allows proteins anchored to these domains to diffuse. Therefore, raft-perturbing manipulations have been shown to alter Sema3A-induced growth cone repulsion, inhibition, and collapse (Guirland et al. 2004).

We have been attempting to construct an in vitro system to investigate the mechanisms underlying innervation of the vasculature using a co-culture system of neuronal cells and vascular smooth muscle cells. We previously demonstrated that catecholaminergic neuronal PC12 cells formed synapse-like contacts with the vascular smooth muscle cell line, SM-3 (Endo et al. 1991). The neurites of the cholinergic neuronal cell line, NG108-15 were found to extend more in co-cultures with SM-3 cells than in monocultures. We identified a repulsive axon guidance molecule, the receptor Nrp-1, among several genes enhanced in NG108-15 cells co-cultured with SM-3 cells (Endo et al. 2004; Kyuka et al. 2008; Kyuka et al. 2006). In the present study, we examined the interaction between NG108-15 cells and SM-3 cells, and investigated changes in the expression and localization of Nrp-1 at the neuronal cell membrane in order to clarify the involvement of Nrp-1 in the innervation and repulsion of cholinergic neuronal cells to their target cells.

Materials and Methods

Cell Lines

NG108-15 a hybrid formed by the Sendai virus-induced fusion of the mouse neuroblastoma clone N18TG-2 and rat glioma clone C6BU-1 (Kato et al. 1981; Nelson et al. 1976; Puro and Nirenberg, 1976).

SM-3 vascular smooth muscle cells from rabbit aortic media (Migas et al. 1997; Sasaki et al. 1989), donated by Dr Sasaki, Kitasato University School of Pharmaceutical Sciences, Tokyo, Japan.

Cell Culture

NG108-15 was maintained in HAT medium (100 μM hypoxanthine, 0.4 μM aminopterin, 16 μM thymidine (Sigma-Aldrich Co. LLC., Tokyo, Japan), and Dulbecco's modified Eagle's medium (DMEM; Life Technologies Japan, Tokyo, Japan) supplemented with 10 % heat-inactivated fetal bovine serum (FBS; Life Technologies)). SM-3 was subcultured in DMEM supplemented with 10 % heat-inactivated FBS. Co-cultures of NG108-15 and SM-3 were performed in serum-free DMEM.

NG108-15 and SM-3 at 2.0×10^4 cells/cm^2, respectively, were monocultured or simply mixed cultured for 5 days with DMEM on collagen type IV-coated coverslips in plastic culture plates for morphological measurements.

NG108-15 (3.0×10^3 cells/cm^2) and SM-3 (1.6×10^3 (LowSM) or 4.0×10^3 (HighSM) cells/cm^2, respectively) were co-cultured for 3 days in DMEM for RT-PCR. NG108-15 cells were monocultured for 3 days in DMEM, 1 mM N^6,2′-O-Dibutyryladenosine 3′,5′-cyclic monophosphate (dbcAMP; SigmaSigma-Aldrich) in DMEM, or 10 % FBS in DMEM. SM-3 cells were solely cultured for 3 days in DMEM.

Regarding colorimetric Nrp-1 immunocytochemistry, NG108-15 (2.0×10^4 cells/cm^2) was monocultured for 3 days in DMEM or in the conditioned media of SM-3, in which SM-3 (initial concentration of 2.0×10^4 cells/cm^2) had been cultured before for 3 days. NG108-15 and SM-3 (1×10^4 cells/cm^2, each) were co-cultured for 3 days in DMEM.

NG108-15 and SM-3 were co-cultured together for 2 days in DMEM at 2.5×10^4 cells/cm^2 each or cultured solely as the control for in situ membrane protein extraction followed by fluorescent cytochemistry.

Synaptophysin Immunostaining, Cell Counting, and Neurite Length Measurements

After fixation with 4 % paraformaldehyde in 0.1 M PBS, cells were permeabilized for 1 h with 0.3 % TX-100 (Nacalai Tesque, Inc, Kyoto, Japan) in PBS, and immunoblocked for 1 h with 1 % skim milk in PBS. Cells were incubated overnight at 4 °C with mouse anti-synaptophysin (1:200, clone SY38, Merck Millipore, Billerica, MA) as the primary antibody. After rinsing, the slices were incubated for 1 h with a biotinylated goat anti-mouse IgG antibody (1:200; Vector Laboratories, Inc., Burlingame, CA) as the secondary antibody, followed by the avidin–biotinylated horseradish peroxidase complex (Vectastain Elite ABC Kit; Vector Laboratories) for 1 h. Immunoreactivity was visualized with 0.2 mg/ml 3,3'-diaminobenzidine tetrahydrochloride and 0.005 % dihydroperoxide in 0.05 M Tris–HCl buffer (pH 7.6). Cells were dehydrated and analyzed after photomicrography. The number of neuronal cells, neuronal cells with extending neurites, and the length of neurites per cell were measured on photomicrographs.

Neuropilin-1 mRNA Quantification

After a brief rinse with Ca^{2+}, Mg^{2+}-free phosphate-buffered saline (PBS), NG108-15 was harvested by repeated flushing with PBS. The remaining SM-3 was harvested

using a treatment with 0.25 % trypsin and 0.02 % ethylenediaminetetraacetic acid (EDTA) in PBS. Cells were collected and total RNA was purified using the High Pure RNA Isolation Kit (Roche Diagnostics K.K., Tokyo, Japan). cDNAs were synthesized by the Transcriptor First Strand cDNA Synthesis Kit using poly-A primer (Roche Diagnostics) and PCR was performed on the GeneAmp® PCR System 2400 (Life Technologies) using the Platinum PCR SuperMix (Life Technologies). Specific primers were designed using Primer-BLAST (NCBI web site, http://www.ncbi.nlm.nih.gov/tools/primer-blast/). Primers were purchased from Japan Bio Services Co., Ltd., Saitama, Japan. The primer set for Nrp-1 common to the mouse and rat was as follows: GCT-GCA-CAA-ATC-TCT-GAA-AC (Forward), ACA-GCA-CAA-CTC-CAC-AGA-CT (Reverse); mouse GAPDH: GGT-TGT-CTC-CTG-CGA-CTT-CA (Forward), TAG-GGC-CTC-TCT-TGC-TCA-GT (Reverse). PCR products were separated on 1 % agarose gels and stained with ethidium bromide. Fluorescent images of the bands were captured and analyzed by Image J software (NIH, http://imagej.nih.gov/ij/).

Immunohistochemical Detection of Neuripilin-1 at the Cell Surface Without Membrane Permeabilization by a Detergent Treatment

After fixation with 4 % paraformaldehyde in 0.1 M PBS, cells were permeabilized for 1 h with 0.3 % TX-100 in PBS (+) or without (-), and immunoblocked for 1 h with 1 % skim milk in PBS. These cells were then incubated overnight at 4 °C with a rabbit anti-Nrp-1 (H-286) antibody (Santa Cruz Biotechnology, Inc, CA: sc-5541) as the primary antibody. After rinsing, the slices were incubated for 1 h with a biotinylated horse anti-rabbit IgG antibody (1:200; Vector Laboratories) as the secondary antibody, followed by the avidin-biotinylated horseradish peroxidase complex (Vectastain Elite ABC Kit; Vector Laboratories) for 1 h. Immunoreactivity was visualized and photographed as described previously for synaptophysin staining. The numbers of Nrp-1-immunopositive growth cones and varicosities were counted on photomicrographs.

Cold Triton X-100 Treatment

In situ protein extraction with cold detergent was performed as described previously (Guirland et al. 2004) with some modifications. Membrane proteins, except for those located on lipid raft domains, were extracted for 4 min at 4 °C with 0.1 % TX-100 in extraction buffer (0.1 M PIPES, 1 mM $MgSO_4$, 2 mM EGTA, 0.1 mM EDTA, 2 M glycerol, pH 6.8).

Methyl-Beta-Cyclodextrin Treatment

Cholesterol depletion was performed as described previously (Ilangumaran and Hoessli 1998). Membrane cholesterol was

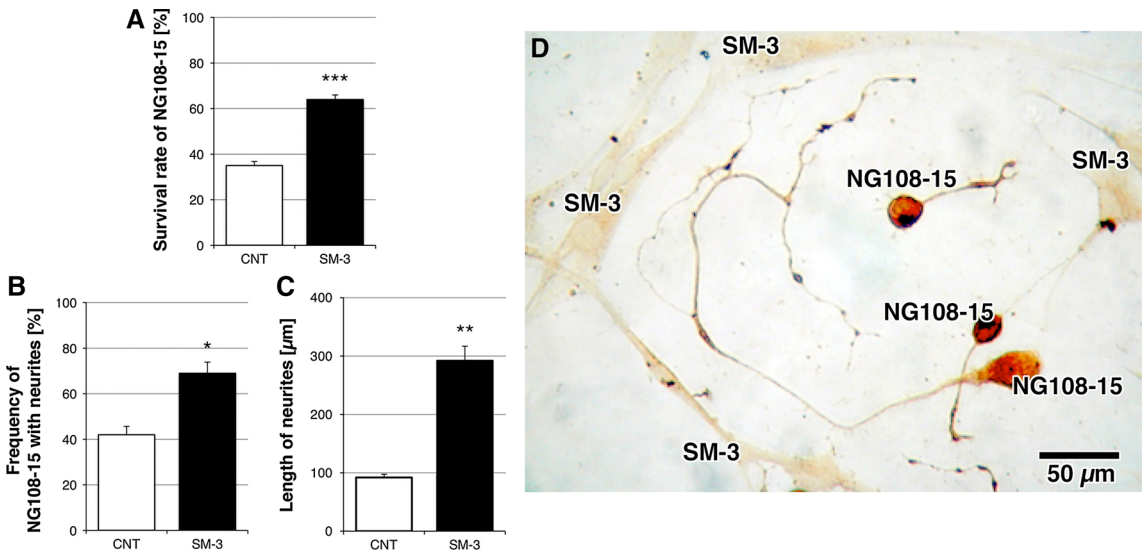

Fig. 1 Effects of a co-culture with SM-3 cells on the viability and neurite extension of NG108-15 cells. **a** *Bar graphs* showing the survival rate of NG108-15 cells in a monoculture (*open bar* CNT; $n = 5$) or co-culture with SM-3 cells (*solid bar* SM-3; $n = 5$). **b** *Bar graphs* showing the frequency of NG108-15 cells with neurites in a monoculture (*open bar* CNT; $n = 6$) or co-culture with SM-3 cells (*solid bar* SM-3; $n = 6$). **c** *Bar graphs* showing the total length of neurites extending from NG108-15 cells in a monoculture (*open bar* CNT; $n = 6$) or co-culture with SM-3 cells (*solid bar* SM-3; $n = 6$). Data are represented as the mean ± standard error of the mean. $*p < 0.05$, $**p < 0.01$, $***p < 0.001$, significantly different from the corresponding CNT, respectively; *t* test. *CNT* control, *SM-3* co-cultures with SM-3 cells. **d** A representative image showing the extension and repulsion-like behavior of neurites in a simple co-culture of NG108-15 cells with SM-3 cells. Cells were immunostained using anti-synaptophysin. *Bar* 50 μm

extracted for 30 min with 10 mM MBCD (a water-soluble cyclic oligomer that extracts cholesterol from the plasma membrane; Wako Pure Chemical Industries, Ltd., Osaka, Japan) in DMEM.

Fluorescent Immunocytochemistry

After fixation with 4 % paraformaldehyde, Nrp-1 was detected using a rabbit anti-Nrp-1 (H-286) antibody (Santa Cruz Biotechnology) and Alexa Fluor 488-conjugated goat anti-rabbit IgG antibody (Life Technologies). Ganglioside has been shown to accumulate in lipid rafts on the cell membrane and regulates the transduction of signals (Harder et al. 1998; Orlandi and Fishman 1998). Ganglioside GM1 (GM1) was detected using 1 μg/ml biotinylated cholera toxin B subunit (List Biological Laboratories Inc., Campbell, CA) and Alexa Fluor 594-conjugated streptavidin (Life Technologies). Fluorescent signals were captured on laser confocal microscopy (Fluoview FV10i, Olympus, Tokyo, Japan). Pixels (2-pixel thick) at the cell fringe of digital images were extracted (Fig. 4f, h, j, Fig. 5f, h, j) using Adobe Photoshop Elements 6.0 software for Mac (Adobe Systems Inc., San Jose, CA). An RGB histogram of each extracted pixel was obtained using Image J software, and the ratio of the green signal (Nrp-1) to the red signal (GM1) (G/R signal ratio) was then calculated at each pixel.

Statistical Analysis

Differences between the mean values of experimental groups were statistically analyzed using the *t* test or Tukey–Kramer multiple comparisons test using InStat software (GraphPad Software, Inc., San Diego, CA).

Results

The viability (Fig. 1a) and number of NG108-15 cells with extending neurites (Fig. 1b) were more than 1.5-fold higher in mixed-cultures with SM-3 cells than in monocultures. The total length of neurites emerging from NG108-15 cells was twofold longer in mixed-cultures than in monocultures (Fig. 1c). Regarding synaptophysin immunostaining, NG108-15 cell bodies and neurites, especially varicosities and growth cones, were intensely immunopositive. Faint non-specific staining was observed in SM-3 cells. NG108-15 cells co-cultured with SM-3 cells frequently extended their neurites; however, several neurites were repelled from SM-3 cells (Fig. 1d).

RT-PCR revealed that mouse and rat Nrp-1 mRNA expression levels (standardized by mouse GAPDH mRNA expression) were approximately 2-fold higher in NG108-15 cells co-cultured with SM-3 cells than in monocultures (Fig. 2a–c).

Regarding Nrp-1 immunocytochemistry, TX100 permeabilization showed Nrp-1 immunoreactivities in approximately 70–80 % of the growth cones and varicosities of NG108-15 cells in monocultures (NG), cultures with the conditioned media of SM-3 cells (NG + CM), and co-cultures with SM-3 cells (NG + SM) (Fig. 3a–c, g (+), h (+)). Furthermore, Nrp-1 immunocytochemistry without TX100 permeabilization showed immunoreactivities in only approximately 15–50 % of the growth cones and varicosities of NG108-15 cells in these groups (Fig. 3d–f, g (−), h (−)). The number of Nrp-1-immunopositive growth cones was significantly larger in the NG + SM group or NG + CM group than that in the NG group (Fig. 3g (−)), whereas no significant differences were observed in the number of Nrp-1-immunopositive varicosities between the three groups (Fig. 3h (−)).

Cell cultures were subjected to the extraction of proteins soluble to cold TX100 or cholesterol depletion by the MBCD treatment in situ. In monocultures, neither the

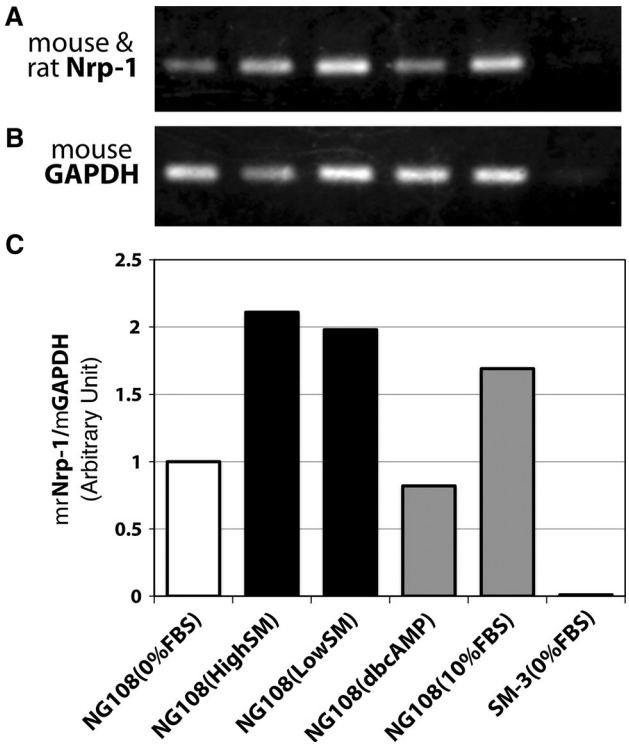

Fig. 2 Neuropilin-1 mRNA expression in NG108-15 cells (and SM-3 cells) under several culture conditions. **a** Fluorescent image showing representative bands of the RT-PCR products for mouse and rat Nrp-1 mRNA, electrophoresed on a 1 % agarose gel. **b** Bands of the PCR products for mouse GAPDH mRNA. **c** *Bar graphs* showing the relative expression of Nrp-1 mRNA normalized by GAPDH. *Nrp-1* neuropilin-1, *GAPDH* glyceraldehyde-3-phosphate dehydrogenase. *dbcAMP* 1 mM N^6,2′-O-Dibutyryladenosine 3′,5′-cyclic monophosphate in DMEM, *0 %FBS* monoculture in serum-free DMEM, *HighSM* co-culture with SM-3 (4.0×10^3 cells/cm^2) in DMEM, *LowSM* co-culture with SM-3 (1.6×10^3 cells/cm^2) in DMEM, *10 %FBS* monoculture in DMEM supplemented with 10 %FBS

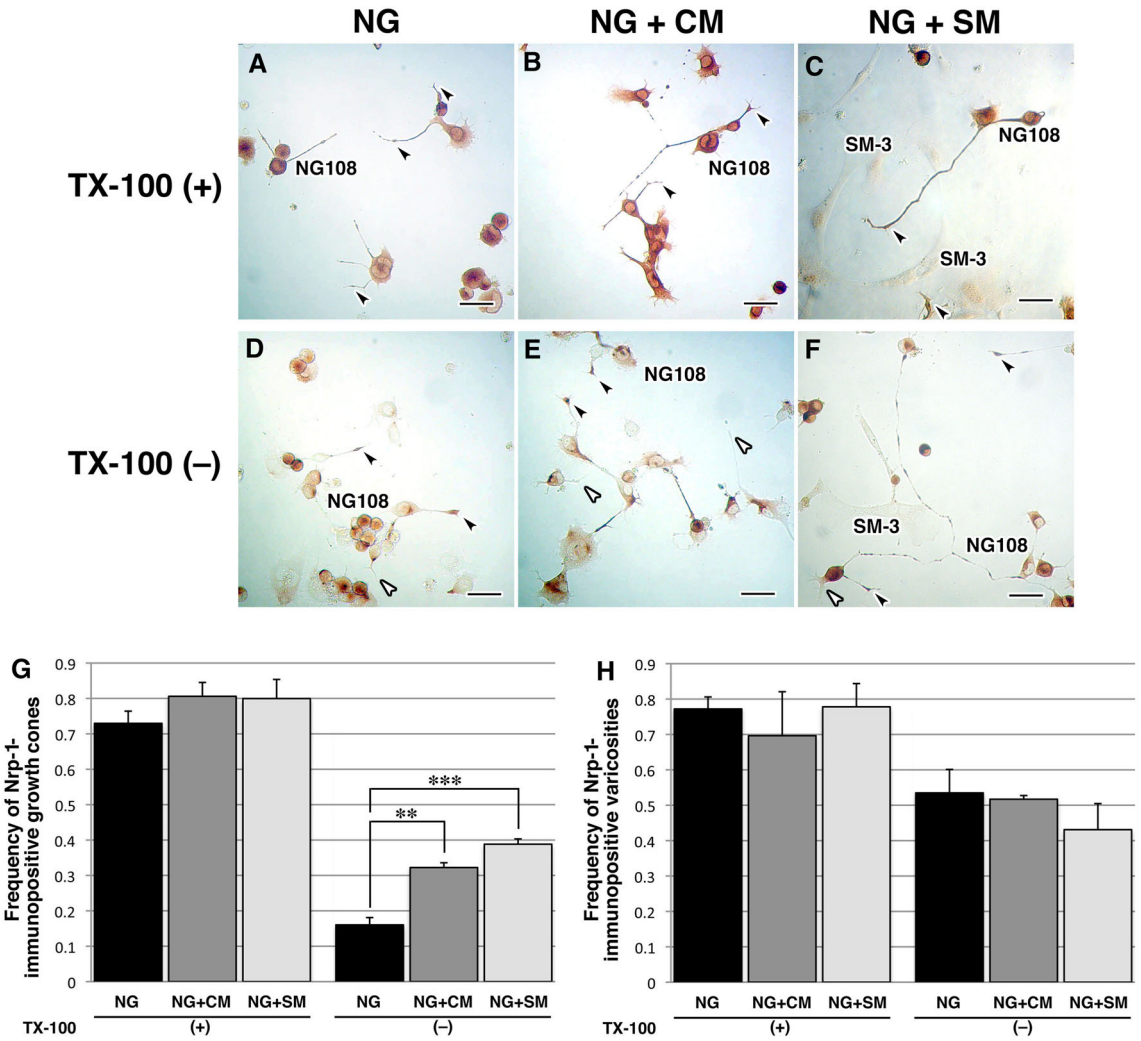

Fig. 3 Whole cell or cell surface detection of neuropilin-1 in NG108-15 cells. **a–c** Photomicrographs showing the whole cellular distribution of Nrp-1 with TX-100 permeabilization (TX-100 (+)). **d–f** Photomicrographs showing the cell surface distribution of Nrp-1 without TX-100 permeabilization (TX-100 (−)). *Solid arrowheads* Nrp-1-immunopositive growth cones. *Open arrowheads* Nrp-1-immunonegative growth cones. *Bars* 50 µm. **g**, **h** *Bar graphs* showing the frequencies of Nrp-1-immunopositive growth cones (**g**) and varicosities (**h**), as assessed by immunocytochemistry combined with (+) or without (−) TX-100 permeabilization. In all groups, $n = 3$. Data are represented as the mean ± standard error of the mean. $^{**}p < 0.01$, $^{***}p < 0.001$ versus Cont or TX100; Tukey–Kramer multiple comparisons test. *NG* NG108-15 monocultures, *NG + CM* NG108-15 cells cultured with the conditioned media of SM-3 cells, *NG + SM* NG108-15 cells co-cultured with SM-3 cells

treatment of cells with cold TX100 nor the treatment with MBCD altered the ratio of fluorescent signals for Nrp-1 and GM1 at the cell surface of NG108-15 cells (Fig. 4a–k). In co-cultures with SM-3, the surface Nrp-1/GM1 ratio in non-treated NG108-15 cells was higher than that in monocultures, and the MBCD treatment significantly decreased the Nrp-1/GM1 ratio at the cell surface of NG108-15 cells, whereas the cold TX100 treatment did not (Fig. 4a'–k').

Discussion

We have examined here the interaction between cholinergic neuronal cells and vascular smooth muscle cells, and identified changes in the expression and localization of Nrp-1 in the neuronal cells co-cultured with smooth muscle cells.

We demonstrated that cell viability, neurites extension from NG108-15 cells, and Nrp-1 mRNA expression were significantly promoted in co-cultures with SM-3, which must produce unidentified growth factors and axon guidance factors.

TX-100 permeabilization allowed the distribution of target molecules at the cell surface and intracellularly to be visualized simultaneously, whereas extracellular epitope-recognizing antibody-using immunocytochemistry with no permeabilizing treatment enabled the cell surface localization to be visualized. The conditioned medium of SM-3

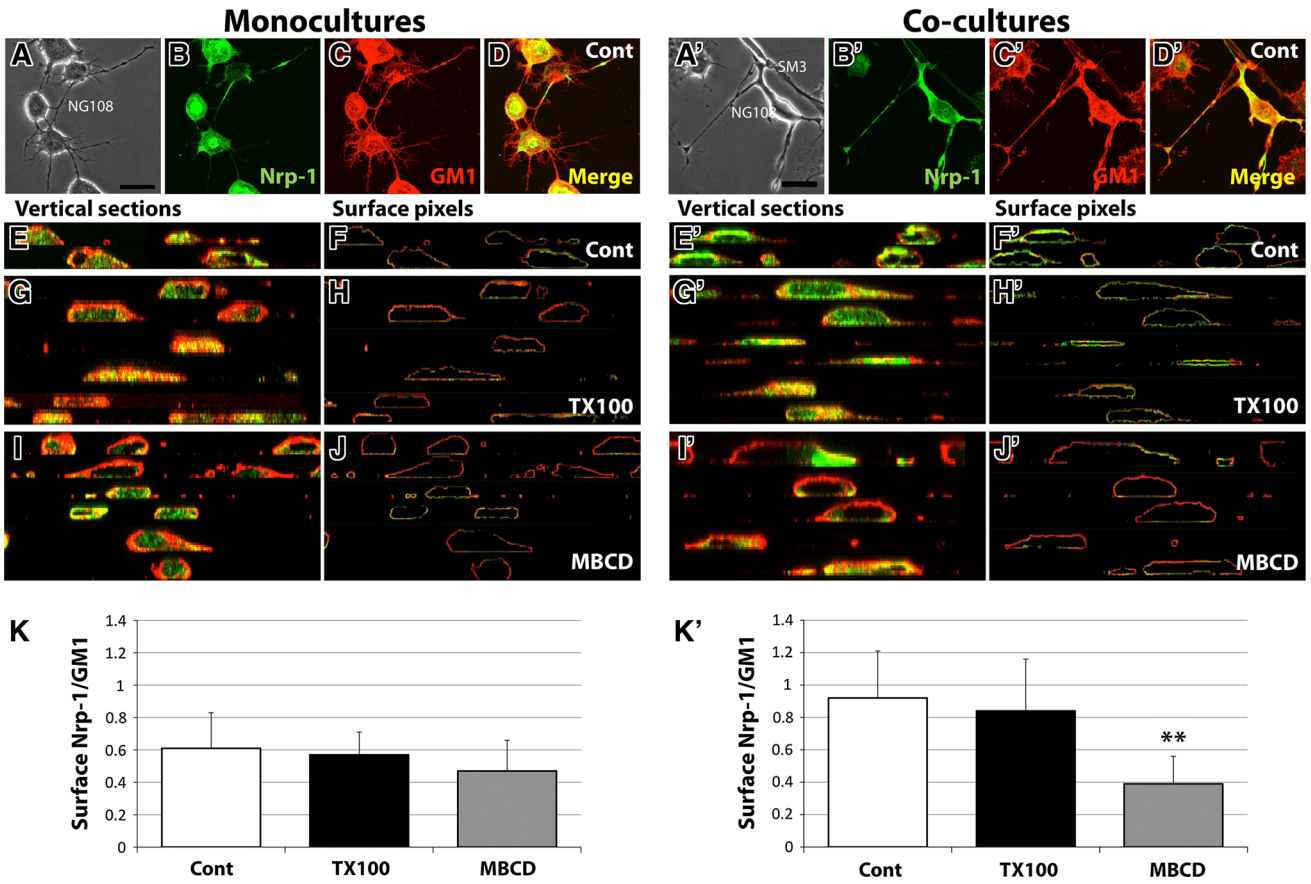

Fig. 4 Neuropilin-1 and ganglioside GM1 in NG108-15 monocultures and co-cultures with SM-3 cells. **a–d**, **a'–d'** Confocal photomicrographs showing Nrp-1 (*green*) and GM1 (*red*) fluorescence in NG108-15 cells with no treatment (Control). **a**, **a'** Phase contrast image. **b**, **b'** Localization of Nrp-1. **c**, **c'** Localization of GM1. **d**, **d'** Merged image. **e–j**, **e'–j'** Confocal photomicrographs showing Nrp-1 and GM1 in vertical sections (**e**, **g**, **i**, **e'**, **g'**, **i'**), and extracted pixels at the cell surface (**f**, **h**, **j**, **f'**, **h'**, **j'**). **e**, **f**, **e'**, **f'** Non-treated control. **g**, **h**, **g'**, **h'** Treated with cold TX-100. **i**, **j**, **i'**, **j'** Treated with MBCD. **k**, **k'** *Bar graphs* showing the ratio of fluorescence for Nrp-1 (*green*) to GM1 (*red*) in the pixels at the cell surface of NG108-15. Data are represented as the mean ± standard deviation. No significant differences were observed in the mean values among the three groups ($n = 6$, 11, 14, respectively; $p > 0.05$, ANOVA) in K. The mean value of the MBCD group ($n = 10$) was significantly lower than that of Cont ($n = 7$) or the TX100 group ($n = 10$) in K'. $^{**}p < 0.01$ versus Cont or TX100, Tukey–Kramer multiple comparisons test. *Cont* Control, *TX100* Triton X-100, *MBCD* methyl-beta-cyclodextrin (Color figure online)

cells as well as co-cultures with SM-3 cells increased Nrp-1 on the surface of the growth cones, but not on the varicosities of neuronal NG108-15 cells, indicating that NG108-15 cells can respond to some soluble factors secreted from SM-3 cells in order to translocate Nrp-1 to the surface of growth cones, suggesting a specific role of Nrp-1 in axon guidance (Nangle and Keast 2011; Shelly et al. 2011; Zylbersztejn et al. 2012).

In co-cultures with SM-3 cells, the signal ratio of Nrp-1/GM1 at the cell surface of NG108-15 cells was higher than that in monocultures. The MBCD treatment significantly decreased the Nrp-1/GM1 ratio at the cell surface of NG108-15 cells, whereas the cold TX100 treatment did not. The results suggest that Nrp-1 have shifted its localization onto lipid rafts within the plasma membrane when NG108-15 cells were co-cultured with SM-3 cells. Therefore, reductions in the amount of cholesterol affected Nrp-1 in the plasma membrane, suggesting that most Nrp-1 translocated have been incorporated into the lipid raft. The translocation of Nrp-1 to the lipid raft domains may play a role in the extension of NG108-15 neurites and repulsion-like behavior against SM-3 cells or may indicate the functional enhancement of Nrp-1 (Guirland et al. 2004; Guirland and Zheng 2007; Kamiguchi 2006).

In most vasculature, varicose axons pass through or terminate at the adventitial medial border and nerve fibers rarely enter into the medial smooth muscle layer (Burnstock 2008). The chemorepulsive system using Nrp-1 may be essentially involved in the autonomic vascular innervation process, and may also characterize the differences between sympathetic and parasympathetic vascular innervations (Amiya et al. 2014; Bevan and Brayden 1987; Burnstock 2008).

The dynamics of Nrp-1 on growth cones or varicosities need to be examined in more detail in order confirm

whether the disruption of Nrp-1 expression or lipid rafts affects the neurite repulsion of NG108-15 cells in co-cultures with SM-3 cells. The critical soluble factors in this system also need to be identified. VSMCs have been suggested to secrete activins, angiotensins, endothelins, fibroblast growth factors (FGFs), hepatocyte growth factor (HGF), insulin-like growth factors (IGFs), interleukins, platelet-derived growth factors (PDGFs), VEGFs, and reactive oxygen species (Berk 2001; Chen et al. 2008; Marko and Damon 2008).

In conclusion, vascular smooth muscle cells may promote cell viability, neurite extension, and Nrp-1 mRNA expression in cholinergic neurons via some soluble factors, but may also induce a contact-repulsive effect to cholinergic neurites, but not catecholaminergic neurites. Furthermore, Nrp-1 shifted its localization onto the cell surface of growth cones, particularly putative raft domains in the plasma membrane. Thus, our simplified co-culture system using vascular smooth muscle cells and the cholinergic neuronal cell line as well as catecholaminergic cell line will be useful for further investigations on the cytological, molecular biological, and physiological bases of the mechanisms underlying autonomic innervations.

Acknowledgments We appreciate Dr. Katsutoshi Taguchi, The Department of Basic Geriatrics, Kyoto Prefectural University of Medicine, Kyoto, Japan for his helpful advice regarding the central experimental methodology.

References

Amiya E, Watanabe M, Komuro I (2014) The Relationship between vascular function and the autonomic nervous system. Ann Vasc Dis 7:109–119

Bates D, Taylor GI, Minichiello J, Farlie P, Cichowitz A, Watson N, Klagsbrun M, Mamluk R, Newgreen DF (2003) Neurovascular congruence results from a shared patterning mechanism that utilizes semaphorin3A and neuropilin-1. Dev Biol 255:77–98

Berk BC (2001) Vascular smooth muscle growth: autocrine growth mechanisms. Physiol Rev 81:999–1030

Bevan JA, Brayden JE (1987) Nonadrenergic neural vasodilator mechanisms. Circ Res 60:309–326

Brunet I, Gordon E, Han J, Cristofaro B, Broqueres-You D, Liu C, Bouvree K, Zhang J, del Toro R, Mathivet T, Larrivee B, Jagu J, Pibouin-Fragner L, Pardanaud L, Machado MJ, Kennedy TE, Zhuang Z, Simons M, Levy BI, Tessier-Lavigne M, Grenz A, Eltzschig H, Eichmann A (2014) Netrin-1 controls sympathetic arterial innervation. J Clin Invest 124:3230–3240

Burnstock G (2008) Non-synaptic transmission at autonomic neuroeffector junctions. Neurochem Int 52:14–25

Chen XL, Chen ZS, Ding Z, Dong C, Guo H, Gong NQ (2008) Antisense extracellular signal-regulated kinase-2 gene therapy inhibits platelet-derived growth factor-induced proliferation, migration and transforming growth factor-beta(1) expression in vascular smooth muscle cells and attenuates transplant vasculopathy. Transpl Int 21:30–38

Endo Y, Maruyama T, Sasaki Y (1991) Coculture of neural and smooth-muscle cell-lines—a model for the peripheral autonomic nervous-system. Biomed Res Tokyo 12:211–214

Endo Y, Matsusaka M, Yoshimura R, Ohara O (2004) The effects of outgrowth of neurites and adhesive repulsion by cultured vascular smooth muscle cells. Zoolog Sci 21:1279

Enomoto H, Crawford PA, Gorodinsky A, Heuckeroth RO, Johnson EM Jr, Milbrandt J (2001) RET signaling is essential for migration, axonal growth and axon guidance of developing sympathetic neurons. Development 128:3963–3974

Foster LJ, De Hoog CL, Mann M (2003) Unbiased quantitative proteomics of lipid rafts reveals high specificity for signaling factors. Proc Natl Acad Sci USA 100:5813–5818

Fujisawa H, Kitsukawa T, Kawakami A, Takagi S, Shimizu M, Hirata T (1997) Roles of a neuronal cell-surface molecule, neuropilin, in nerve fiber fasciculation and guidance. Cell Tissue Res 290:465–470

Grider MH, Park D, Spencer DM, Shine HD (2009) Lipid raft-targeted Akt promotes axonal branching and growth cone expansion via mTOR and Rac1, respectively. J Neurosci Res 87:3033–3042

Guirland C, Zheng JQ (2007) Membrane lipid rafts and their role in axon guidance. Adv Exp Med Biol 621:144–155

Guirland C, Suzuki S, Kojima M, Lu B, Zheng JQ (2004) Lipid rafts mediate chemotropic guidance of nerve growth cones. Neuron 42:51–62

Harder T, Scheiffele P, Verkade P, Simons K (1998) Lipid domain structure of the plasma membrane revealed by patching of membrane components. J Cell Biol 141:929–942

He Z, Tessier-Lavigne M (1997) Neuropilin is a receptor for the axonal chemorepellent semaphorin III. Cell 90:739–751

Honma Y, Araki T, Gianino S, Bruce A, Heuckeroth R, Johnson E, Milbrandt J (2002) Artemin is a vascular-derived neurotropic factor for developing sympathetic neurons. Neuron 35:267–282

Hooper NM (1999) Detergent-insoluble glycosphingolipid/cholesterol-rich membrane domains, lipid rafts and caveolae (review). Mol Memb Biol 16:145–156

Ilangumaran S, Hoessli DC (1998) Effects of cholesterol depletion by cyclodextrin on the sphingolipid microdomains of the plasma membrane. Biochem J 335(Pt 2):433–440

Kamiguchi H (2006) The region-specific activities of lipid rafts during axon growth and guidance. J Neurochem 98:330–335

Kato K, Higashida H, Umeda Y, Suzuki F, Tanaka T (1981) Regulation of neuron-specific enolase in NG108-15 hybrid cells and C6BU-1 glioma cells. Biochim Biophys Acta 660:30–35

Kitsukawa T, Shimizu M, Sanbo M, Hirata T, Taniguchi M, Bekku Y, Yagi T, Fujisawa H (1997) Neuropilin-semaphorin III/D-mediated chemorepulsive signals play a crucial role in peripheral nerve projection in mice. Neuron 19:995–1005

Kolodkin AL, Levengood DV, Rowe EG, Tai YT, Giger RJ, Ginty DD (1997) Neuropilin is a semaphorin III receptor. Cell 90:753–762

Kuruvilla R, Zweifel LS, Glebova NO, Lonze BE, Valdez G, Ye H, Ginty DD (2004) A neurotrophin signaling cascade coordinates sympathetic neuron development through differential control of TrkA trafficking and retrograde signaling. Cell 118:243–255

Kyuka A, Yoshimura R, Endo Y (2006) Subcellular localization of neuropilin in NG108 cells co-cultured with target cells. Neurosci Res 55:S182–S182

Kyuka A, Fushiki D, Yoshimura R, Nishida T, Fujisawa H, Endo Y (2008) 3D tomographic image analysis of axonal guidance molecule receptors (neuropilin and plexin) in NG108 cells by UHVEM. Neurosci Res 61:S161–S161

Long JB, Jay SM, Segal SS, Madri JA (2009) VEGF-A and semaphorin3A: modulators of vascular sympathetic innervation. Dev Biol 334:119–132

Makita T, Sucov HM, Gariepy CE, Yanagisawa M, Ginty DD (2008) Endothelins are vascular-derived axonal guidance cues for developing sympathetic neurons. Nature 452:759–763

Marko SB, Damon DH (2008) VEGF promotes vascular sympathetic innervation. Am J Physiol Heart Circ Physiol 294:H2646–H2652

Migas I, Chuang M, Sasaki Y, Severson DL (1997) Diacylglycerol metabolism in SM-3 smooth muscle cells. Can J Physiol Pharmacol 75:1249–1256

Nangle MR, Keast JR (2011) Semaphorin 3A inhibits growth of adult sympathetic and parasympathetic neurones via distinct cyclic nucleotide signalling pathways. Br J Pharmacol 162:1083–1095

Nelson P, Christian C, Nirenberg M (1976) Synapse formation between clonal neuroblastoma X glioma hybrid cells and striated muscle cells. Proc Natl Acad Sci USA 73:123–127

Orlandi PA, Fishman PH (1998) Filipin-dependent inhibition of cholera toxin: evidence for toxin internalization and activation through caveolae-like domains. J Cell Biol 141:905–915

Pike LJ, Miller JM (1998) Cholesterol depletion delocalizes phosphatidylinositol bisphosphate and inhibits hormone-stimulated phosphatidylinositol turnover. J Biol Chem 273:22298–22304

Puro DG, Nirenberg M (1976) On the specificity of synapse formation. Proc Natl Acad Sci USA 73:3544–3548

Sasaki Y, Uchida T, Sasaki Y (1989) A variant derived from rabbit aortic smooth muscle: phenotype modulation and restoration of smooth muscle characteristics in cells in culture. J Biochem 106:1009–1018

Shelly M, Cancedda L, Lim BK, Popescu AT, Cheng PL, Gao H, Poo MM (2011) Semaphorin3A regulates neuronal polarization by suppressing axon formation and promoting dendrite growth. Neuron 71:433–446

Simons K, Ikonen E (1997) Functional rafts in cell membranes. Nature 387:569–572

Verkade P, Simons K (1997) Robert Feulgen Lecture 1997. Lipid microdomains and membrane trafficking in mammalian cells. Histochem Cell Biol 108:211–220

Zylbersztejn K, Petkovic M, Burgo A, Deck M, Garel S, Marcos S, Bloch-Gallego E, Nothias F, Serini G, Bagnard D, Binz T, Galli T (2012) The vesicular SNARE synaptobrevin is required for semaphorin 3A axonal repulsion. J Cell Biol 196:37–46